The Antimicrobial Peptide CRAMP Is Essential for Colon Homeostasis by Maintaining Microbiota Balance

Teizo Yoshimura,[*,†] Mairi H. McLean,[*,‡] Amiran K. Dzutsev,[*] Xiaohong Yao,[§] Keqiang Chen,[*] Jiaqiang Huang,[*,¶] Wanghua Gong,[‖] Jiamin Zhou,[*] Yi Xiang,[*] Jonathan H. Badger,[*] Colm O'hUigin,[*] Vishal Thovarai,[‖] Lino Tessarollo,[#] Scott K. Durum,[*] Giorgio Trinchieri,[*] Xiu-wu Bian,[§] and Ji Ming Wang[*]

Commensal bacteria are critical for physiological functions in the gut, and dysbiosis in the gut may cause diseases. In this article, we report that mice deficient in cathelin-related antimicrobial peptide (CRAMP) were defective in the development of colon mucosa and highly sensitive to dextran sulfate sodium (DSS)-elicited colitis, as well as azoxymethane-mediated carcinogenesis. Pretreatment of CRAMP$^{-/-}$ mice with antibiotics markedly reduced the severity of DSS-induced colitis, suggesting CRAMP as a limiting factor on dysbiosis in the colon. This was supported by observations that wild-type (WT) mice cohoused with CRAMP$^{-/-}$ mice became highly sensitive to DSS-induced colitis, and the composition of fecal microbiota was skewed by CRAMP deficiency. In particular, several bacterial species that are typically found in oral microbiota, such as *Mogibacterium neglectum*, *Desulfovibrio piger*, and *Desulfomicrobium orale*, were increased in feces of CRAMP$^{-/-}$ mice and were transferred to WT mice during cohousing. When littermates of CRAMP$^{+/-}$ parents were examined, the composition of the fecal microbiota of WT pups and heterozygous parents was similar. In contrast, although the difference in fecal microbiota between CRAMP$^{-/-}$ and WT pups was small early on after weaning and single mouse housing, there was an increasing divergence with prolonged single housing. These results indicate that CRAMP is critical in maintaining colon microbiota balance and supports mucosal homeostasis, anti-inflammatory responses, and protection from carcinogenesis. *The Journal of Immunology*, 2018, 200: 2174–2185.

Commensal bacteria are involved in various physiological functions in the gut, and microbial imbalance (dysbiosis) is implicated in pathological changes (1). The microbiota in the colon is separated from the host compartment by a single layer of epithelial cells, which has the capacity to respond to and control potential pathogenic threats from commensal bacteria (2, 3). In addition to the pattern recognition receptors, such as TLRs and related NOD proteins that recognize microbe-associated molecular patterns, formyl peptide receptors (FPRs; Fprs for mouse), a subfamily of the seven-transmembrane G protein–coupled chemoattractant receptors, also interact with pathogen- and damage-associated chemotactic molecules (4–6).

Human FPRs and mouse Fprs are expressed by colonic epithelial cells and participate in important pathophysiological responses. Mice deficient in Fpr2 showed shortened colon crypt length, with reduced epithelial cell proliferation, reduction in the severity of acute inflammatory responses to dextran sulfate sodium (DSS) but delayed mucosal restoration after injury, increased chemically induced tumorigenesis, and increased bacterial abundance in the colon (7). Thus, Fpr2 contributes to colonic epithelial homeostasis, inflammation, and tumorigenesis in mice, presumably by interacting with commensal bacterial products; however, the capacity of Fpr2 (or human FPR2) to recognize endogenous ligands in the colon remains unclear.

One of the human FPR2 ligands, the antimicrobial peptide LL-37, is highly expressed by colon epithelia (8). The mouse ortholog of LL-37, cathelin-related antimicrobial peptide (CRAMP) (9), is expressed in epithelial cells of small intestine in the neonatal period (nondetectable by 21 d) and confers significant protection to the newborn from infection by the enteric pathogen *Listeria monocytogenes* (10). Intrarectal administration of exogenous CRAMP alleviated DSS-induced colitis by preserving the mucous layer, reducing proinflammatory cytokine production, and suppressing epithelial apoptosis (11). Oral administration of CRAMP-transformed *Lactococcus lactis* ameliorated DSS-induced colitis in mice (12). In addition, CRAMP mediates the migration of

*Cancer and Inflammation Program, Center for Cancer Research, National Cancer Institute at Frederick, Frederick, MD 21702; †Department of Pathology and Experimental Medicine, Graduate School of Medicine, Dentistry and Pharmaceutical Sciences, Okayama University, Okayama 700-8558, Japan; ‡School of Medicine, Medical Sciences and Nutrition, University of Aberdeen, Aberdeen AB25 2ZD, United Kingdom; §Institute of Pathology and Southwest Cancer Center, Third Military Medical University, Chongqing 400038, China; ¶College of Life Sciences and Bioengineering, School of Science, Beijing Jiaotong University, Beijing 100044, China; ‖Basic Science Program, Leidos Biomedical Research, Inc., Frederick National Laboratory for Cancer Research, Frederick, MD 21702; and #Mouse Cancer Genetics Program, Center for Cancer Research, National Cancer Institute at Frederick, Frederick, MD 21702

ORCIDs: 0000-0002-7443-2653 (M.H.M.); 0000-0002-4423-7072 (X.Y.); 0000-0002-5662-423X (J.H.B.).

Address correspondence and reprint requests to Dr. Ji Ming Wang or Dr. Teizo Yoshimura, Building 560, Room 31-76, Cancer and Inflammation Program, Center for Cancer Research, National Cancer Institute at Frederick, Frederick, MD 21702 (J.M.W.) or Department of Pathology and Experimental Medicine, Graduate School of Medicine, Dentistry and Pharmaceutical Sciences, Okayama University, 2-5-1 Shikata, Kita-ku, Okayama 700-8558, Japan (T.Y.). E-mail addresses: wangji@mail.nih.gov (J.M.W.) or yoshimut@okayama-u.ac.jp (T.Y.)

The online version of this article contains supplemental material.

Abbreviations used in this article: ABX, antibiotics; AOM, azoxymethane; BM, bone marrow; CRAMP, cathelin-related antimicrobial peptide; DSS, dextran sulfate sodium; FPR/fpr, formyl peptide receptor; IHC, immunohistochemistry; ILA, isolated lymphoid aggregate; OUT, operational taxonomic unit; WT, wild-type.

leukocytes and promotes innate and adaptive immune responses in mice by interacting with Fpr2 (9, 13).

Collectively, these results led us to hypothesize that endogenously produced CRAMP may actively participate in the pathophysiological processes in the colon by maintaining the homeostasis of microbiota. We tested this hypothesis by examining newly generated CRAMP$^{-/-}$ mice and demonstrate that CRAMP plays a critical role in colonic homeostasis, inflammation, and carcinogenesis by regulating microbiota balance.

Materials and Methods
Mice

Wild-type (WT) C57BL/6NCr mice were originally purchased from Charles River (Frederick, MD) and used as breeders. Systemic CRAMP$^{-/-}$ and CRAMP$^{flox/flox}$ mice were generated as detailed in Supplemental Fig. 1. All mice used in this study were produced and maintained in the same room in the animal facility at the National Cancer Institute at Frederick. For colitis experiments, mice were transferred to another room on the same floor just before the experiment and kept there until the end. Six- to twelve-week-old male mice were used throughout the study. The experimental protocols were approved by the Frederick National Laboratory for Cancer Research Animal Care and Use Committee, and all experiments were performed in accordance with relevant guidelines and regulations.

To generate littermates, CRAMP heterozygotes (CRAMP$^{+/-}$) were generated by crossing CRAMP$^{-/-}$ mice to WT mice, and several cages of CRAMP$^{+/-}$ breeding pairs were set up. Pups were genotyped and weaned at 4 wk. WT or CRAMP$^{-/-}$ pups were single housed for up to 13 wk, and feces were collected.

Induction of colitis and carcinogenesis

Colitis was induced by administration of different concentrations (1.5–3%) of DSS (40,000–50,000 Da, Lot number 4288597; Affymetrix, Cleveland, OH) in drinking water for 5 d. Mice were allowed to recover on normal drinking water for an additional 4–14 d. The disease activity index was calculated as previously described (7, 14). Mice were euthanized when they lost 20% of their original weight or when they developed prolapse. In a few experiments, mice were euthanized when they lost 35% of their original weight.

To induce colitis-associated tumors, mice received an i.p. injection of 12.5 mg/kg azoxymethane (AOM; product number A5486; Sigma-Aldrich, St. Louis, MO) (15). Mice were exposed 7 d later to 1% DSS in drinking water for 1 wk, followed by 2 wk of normal drinking water. The DSS treatment was repeated for three cycles. All mice were euthanized 12 wk after the AOM injection when one of them developed prolapse. Colons were excised, flushed with PBS, and opened longitudinally. The size of each tumor was measured, and the number of tumors was counted.

Antibiotic treatment and cohousing

Mice were given fresh drinking water containing a mixture of antibiotics (ABX) (vancomycin, imipenem/cilastatin, and neomycin) every 2 d for 3 wk, as previously described (16). DSS was dissolved in the ABX-containing drinking water. With regard to cohousing, several cages containing two WT and two CRAMP$^{-/-}$ mice were set up at the time of weaning (4 wk of age) and maintained for 4 wk prior to use.

BrdU incorporation

To examine DNA synthesis, mice were injected i.p. with 2 mg of BrdU (BD Biosciences). Mice were euthanized 2 or 24 h after BrdU injection, and the colons were harvested. The incorporation of BrdU was examined by immunohistochemistry (IHC), as described below.

Intestinal permeability

Intestinal permeability was determined by assessing the absorption of FITC-dextran, as previously described (17), and per the manufacturer's protocol. Mice were fasted for 4 h and orally gavaged with 20 ml/kg FITC-Dextran, 40 kDa (catalog number 4009, 25 mg/ml; Chondrex). Following an additional 3-h fasting period, mice were euthanized, and blood was collected by cardiac puncture. Plasma was diluted 2-fold in PBS, placed in black-walled clear-bottom 96-well plates (product number 3603; Corning Costar), and assessed for fluorescence intensity at excitation 490 nm and emission 520 nm on a fluorescent plate reader. Concentration of plasma FITC-dextran was determined by comparison with a standard curve prepared with stock FITC-dextran diluted with normal mouse plasma. Five mice per group were used. Data are presented as mean ± SEM.

Histological analyses

Mouse colons were fixed in neutral buffered formalin and embedded in paraffin. Sections (3 μm) were prepared and stained with H&E. IHC for CD3, B220, and F4/80, to identify T cells, B cells, and macrophages, respectively, was performed on a Leica Biosystems Bond automated stainer. Sections were blocked with 2% normal rabbit serum (Vector Laboratories) for 20 min and subsequently incubated for 30 min with anti-CD3 Ab (AbD Serotec), anti-B220 Ab (BD Biosciences), or anti-F4/80 Ab (eBioscience). Biotinylated secondary Ab (rabbit anti-rat IgG), diluted 1:100 in 1.5% normal rabbit serum, was applied to the slides for 30 min and detected with Intense R Detection (Leica Biosystems). IHC for BrdU was performed manually using anti-BrdU Ab (Invitrogen) and a VECTASTAIN Elite ABC Kit (Standard) (Vector Laboratories).

RNA purification and cDNA synthesis

RNA was extracted from snap-frozen distal colon using an RNeasy Mini Kit (QIAGEN), as per the instructions. Quality and yield were assessed by NanoDrop spectrophotometry. cDNA was synthesized using a QuantiTect Reverse Transcription Kit (catalog number 205310; QIAGEN) with inclusive gDNA Wipeout Buffer. Gene expression was assessed with TaqMan Real-Time PCR Assays and TaqMan Universal PCR MasterMix (catalog number 4304437) on a 7300 Real-Time PCR System (all from Applied Biosystems). Data were analyzed for relative expression using the ddCt method, normalized to HPRT endogenous control. To detect the expression of cytokines and chemokines, colons were placed in RNAlater (Ambion). Total RNA was isolated from colon homogenates using TRIzol Reagent (Invitrogen), precipitated, and then used.

DNA extraction, quantification, and sequencing of fecal bacteria

Fecal DNA was prepared using a DNA Stool Mini Kit (QIAGEN). Fecal samples were sequenced as described earlier (18). Briefly, the V4 fragment of 16S rDNA was amplified by PCR using primers 515F 5′-GTGCCAGCMGCCGCGGTAA-3′ and 806R 5′-GGACTACHVGGGTWTC-TAAT-3′ flanked by p5 and p7 Illumina Sequencing adaptors (p5 and p7), barcode (i5 and i7), pad (to optimize melting temperature), and a link sequence. PCR was done with 200 ng of fecal DNA using AccuPrime High Fidelity Taq Polymerase (Invitrogen), with an initial step at 95˚C for 2 min, followed by 25 cycles of 20 s at 95˚C, 30 s at 55˚C, and 7 min at 72˚C. PCR products were purified and normalized using a SequalPrep Normalization Plate Kit (Invitrogen), and the resultant eluents were pooled together and quantified using an Agilent TapeStation (high-sensitivity DNA kits) and Qubit (DNA). A pooled DNA library from 96 samples was denatured, diluted, and sequenced on an Illumina MiSeq (using a V2 500 cycle kit), according to the manufacturer's protocol. Typically, we obtained ~100,000 high-quality reads per sample. Sequence processing was performed using mothur v.1.30.0. as described in the MiSeq 16S standard operating procedure protocol (18). Briefly, contigs were generated from the R1 and R2 sequences, followed by read assignment to the corresponding barcodes; low-quality sequences and chimeras were removed. Sequences were aligned to the SILVA reference dataset, trimmed to the same length, and clustered to produce operational taxonomic units (OTUs) with >97% similarity. Sequences were also classified using the Ribosomal Database Project and Greengenes reference datasets. Both types of data, classified sequences and binned OTUs, were used in downstream analyses for comparisons between the groups. β diversities (weighted and unweighted UniFrac) and α diversities (Chao and Inverse Simpson Index) were calculated using mothur software. All sequence processing was done using the National Institutes of Health Biowulf Cluster. OTUs and classified reads datasets were normalized to the geometric mean and analyzed using Partek Genomics Suite, version 6.0 (Partek, St. Louis, MO). Statistical analysis was performed using ANOVA, and p values were corrected for multiple comparisons using the q-value test (<0.1). The sequence data used in this study were submitted to the Short Read Archive under accession number PRJNA429251 (https://www.ncbi.nlm.nih.gov/sra/SRP128546).

Statistical analyses

All experiments were performed at least three times with comparable results. Statistical analysis was performed by using the Student t test or log-rank (Mantel–Cox) test using GraphPad Prism 6 (GraphPad Software, San Diego, CA). A value of $p < 0.05$ was considered statistically significant.
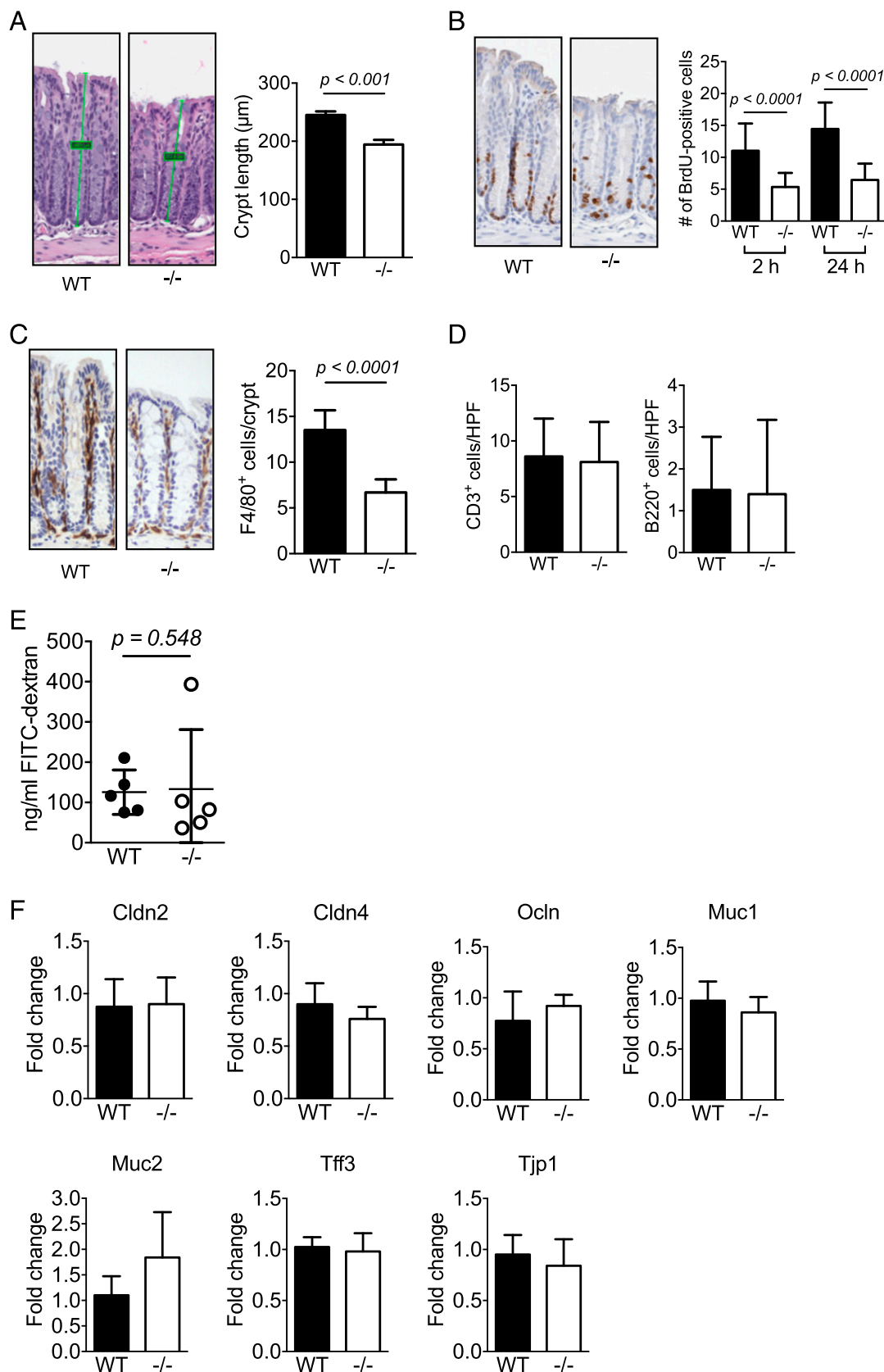
FIGURE 1. CRAMP plays a role in colonic homeostasis. (**A**) Distal sections of colons were obtained from five WT and CRAMP$^{-/-}$ mice, H&E sections were prepared, and the length of colonic crypts (four to nine crypts from each colon) was measured. Data are mean $\pm$ SEM of five mice in each group. (**B**) BrdU was injected i.p. into untreated WT or CRAMP$^{-/-}$ mice. Colons were excised 2 or 24 h after the injection, and the incorporation of BrdU was examined by IHC. BrdU$^+$ cells in 20 crypts per mouse were counted. Two mice per group were used for 2 h, and one mouse per group was used for 24 h. Data are mean $\pm$ SEM. (**C**) The infiltration of macrophages (F4/80$^+$) was examined by IHC. Positive cells in 10 high-power fields (HPFs) were counted. Data are mean $\pm$ SEM per HPF. (A–C) Original magnification $\times$200. (**D**) The infiltration of T cells (CD3$^+$) and B cells (B220$^+$) was examined by IHC. Positive cells in 10 HPFs were counted. Data are mean $\pm$ SEM per HPF. (**E**) Mice were fasted overnight and then dextran-FITC was instilled into the *(Figure legend continues)*

Results

CRAMP is critical for colon homeostasis

To examine whether endogenously produced CRAMP actively participates in pathophysiological processes, in particular, homeostasis, in the colon, we generated CRAMP$^{-/-}$ mice (Supplemental Fig. 1) and examined the colon of naive mice. As shown in Fig. 1A, the length of colonic crypts was significantly shorter in CRAMP$^{-/-}$ mice compared with WT mice. This shortening in CRAMP$^{-/-}$ mice was associated with reduced proliferation of epithelial cells, as demonstrated by significantly decreased BrdU incorporation (Fig. 1B). These results indicate that, in the absence of CRAMP, naive mouse colon epithelial cells are in a hypoproliferative state.

Gut macrophages are normally located in the lamina propria in close proximity to luminal bacteria and regulate inflammatory responses to the bacteria that breach the epithelial layer to protect the mucosa (19). As shown in Fig. 1C, F4/80$^+$ macrophages were detected in subepithelial lamina propria of WT and CRAMP$^{-/-}$ mouse colons; however, the number of F4/80$^+$ macrophages per crypt was significantly reduced in CRAMP$^{-/-}$ colons, whereas the number of CD3$^+$ T cells or B220$^+$ B cells at the same location was similar between WT and CRAMP$^{-/-}$ mice (Fig. 1D). No active inflammation with neutrophil infiltration was detected in WT or CRAMP$^{-/-}$ mouse colons. There was also no sign of increased gut permeability, because the plasma concentration of gavaged FITC (Fig. 1E) and the expression levels of genes critical for barrier functions, including claudin 2 (Cldn2), claudin 4 (Cldn4), occludin (Ocln), trefoil factor 3 (Tff3), mucin1 (Muc1), mucin2 (Muc2), and tight junction protein 1 (Tjp1), were the same in WT and CRAMP$^{-/-}$ mice (Fig. 1F). Thus, epithelial barrier integrity appears to be intact in naive CRAMP$^{-/-}$ mouse colons.

We next examined the number of isolated lymphoid aggregates (ILAs), which are randomly distributed in human and mouse colon and are a key element in mucosal immune regulation (20, 21). A similar number of ILAs was present in the colon of WT and CRAMP$^{-/-}$ mice (Fig. 2A, 2B). However, there was a significant increase in the number of larger ILAs, primarily composed of B220$^+$ B lymphocytes, in the colon of CRAMP$^{-/-}$ mice (Fig. 2A, 2B). These results suggest that CRAMP may play an important role in the immune response in the colon. Therefore, we examined the weight and length of colons of naive WT and CRAMP$^{-/-}$ mice. Although there was no significant difference in the length of colons between WT and CRAMP$^{-/-}$ mice, the colon weight and the weight/length ratio were significantly increased in CRAMP$^{-/-}$ mice (Fig. 2C), suggesting the presence of potentially abnormal and low-level inflammatory responses in the colon of CRAMP$^{-/-}$ mice.

CRAMP$^{-/-}$ mice are highly sensitive to chemically induced colitis and carcinogenesis

We induced acute colitis in WT and CRAMP$^{-/-}$ mice by administering 3% DSS in drinking water. WT mice showed clinical signs of acute colitis, including weight loss, rectal bleeding, and diarrhea, around day 6, and 40% of the mice died by day 8. In contrast, all CRAMP$^{-/-}$ mice showed clinical signs of severe acute colitis by day 5, and 100% of mice died by day 8 (Fig. 3A, left panel). In response to a lower concentration of DSS (2%), all WT mice survived without showing significant signs of colitis,

whereas all CRAMP$^{-/-}$ mice died by day 10 with signs of severe acute colitis (Fig. 3A, right panel). The length of CRAMP$^{-/-}$ mouse colons was significantly shortened by day 4 after 3% DSS intake (Fig. 3B), which was consistent with the signs of acute colitis.

Histologically, the epithelia of CRAMP$^{-/-}$ mouse colon were markedly damaged and necrotic by day 3 and infiltrated by numerous leukocytes, including neutrophils. In comparison, WT mouse colon showed mostly intact epithelia (Fig. 3C). On day 4, the inflammatory responses, including leukocyte infiltration and tissue edema, significantly increased in CRAMP$^{-/-}$ mouse colon compared with WT mouse colon (Fig. 3C). We also detected increased expression of mRNAs encoding proinflammatory cytokines and chemokines, such as TNF-α and CXCL1, in the colon of CRAMP$^{-/-}$ mice 3 d after DSS treatment (Fig. 3D). These results confirm a higher sensitivity of CRAMP$^{-/-}$ mice to DSS-induced colitis, and CRAMP is critical for protecting the colon from inflammatory insults.

We next examined recovery of the colon mucosa following DSS exposure. Mice were given lower concentrations of DSS (1.5%) for 5 d and allowed to recover for an additional 15 d on regular water. As shown in Fig. 4A, CRAMP$^{-/-}$ mice developed severe acute colitis, even at this DSS concentration, and recovered very slowly compared with WT mice. Their weight did not reach the original level by day 37, and the colon length was significantly shorter (Fig. 4B). The mucosa of WT mouse colons showed little histological change compared with normal mucosa, whereas that of CRAMP$^{-/-}$ mouse colons was thickened, with increased epithelial cell proliferation, as indicated by the increased number of BrdU$^+$ cells, and increased leukocyte infiltration, including neutrophils and mononuclear cells (Fig. 4C). When mice were treated with AOM plus three cycles of 1.5% DSS, CRAMP$^{-/-}$ mice developed more numerous colon tumors with larger sizes compared with WT mice (Fig. 4D–F). The length of the colon was also markedly shortened in CRAMP$^{-/-}$ mice (Fig. 4D). Tumors formed in the colon of WT and CRAMP$^{-/-}$ mice were polypoid, and all tumor sections that we examined were diagnosed histologically as adenocarcinoma limited to the mucosa or submucosa (Fig. 4G). Thus, the colon of CRAMP$^{-/-}$ mice readily develops severe chronic colitis with increased epithelial cell proliferation, likely contributing to the development of colon cancer.

Pretreatment with ABX reduces the severity of DSS-induced colitis in CRAMP$^{-/-}$ mice

Intestinal microbiota and their products have been implicated in the pathogenesis of inflammatory bowel disease and DSS-induced colitis in mice. It was previously demonstrated that mucosal destruction caused by DSS occurs without the involvement of the intestinal microbiome, which instead affects the susceptibility and responsiveness to DSS-induced damage (22). Because CRAMP is an antimicrobial peptide, its absence may alter the composition of microbiota, resulting in higher susceptibility of CRAMP$^{-/-}$ mice to DSS. To test this possibility, we pretreated WT and CRAMP$^{-/-}$ mice with a mixture of ABX (16) for 3 wk, followed by administration of 3% DSS in drinking water. As shown in Fig. 5A, ABX treatment significantly rescued WT and CRAMP$^{-/-}$ mice from DSS-induced death; however, CRAMP$^{-/-}$ mice continued to show signs of

stomach. Blood was collected, serum was isolated, and the concentration of FITC was measured. Data are mean ± SD obtained from five mice per group. (**F**) The expression of genes involved in epithelial integrity, including Cldn2, Cldn4, Ocln, Muc1, Muc2, Tff3 and Tjp1, was examined. Data are mean ± SD obtained from five mice per group.
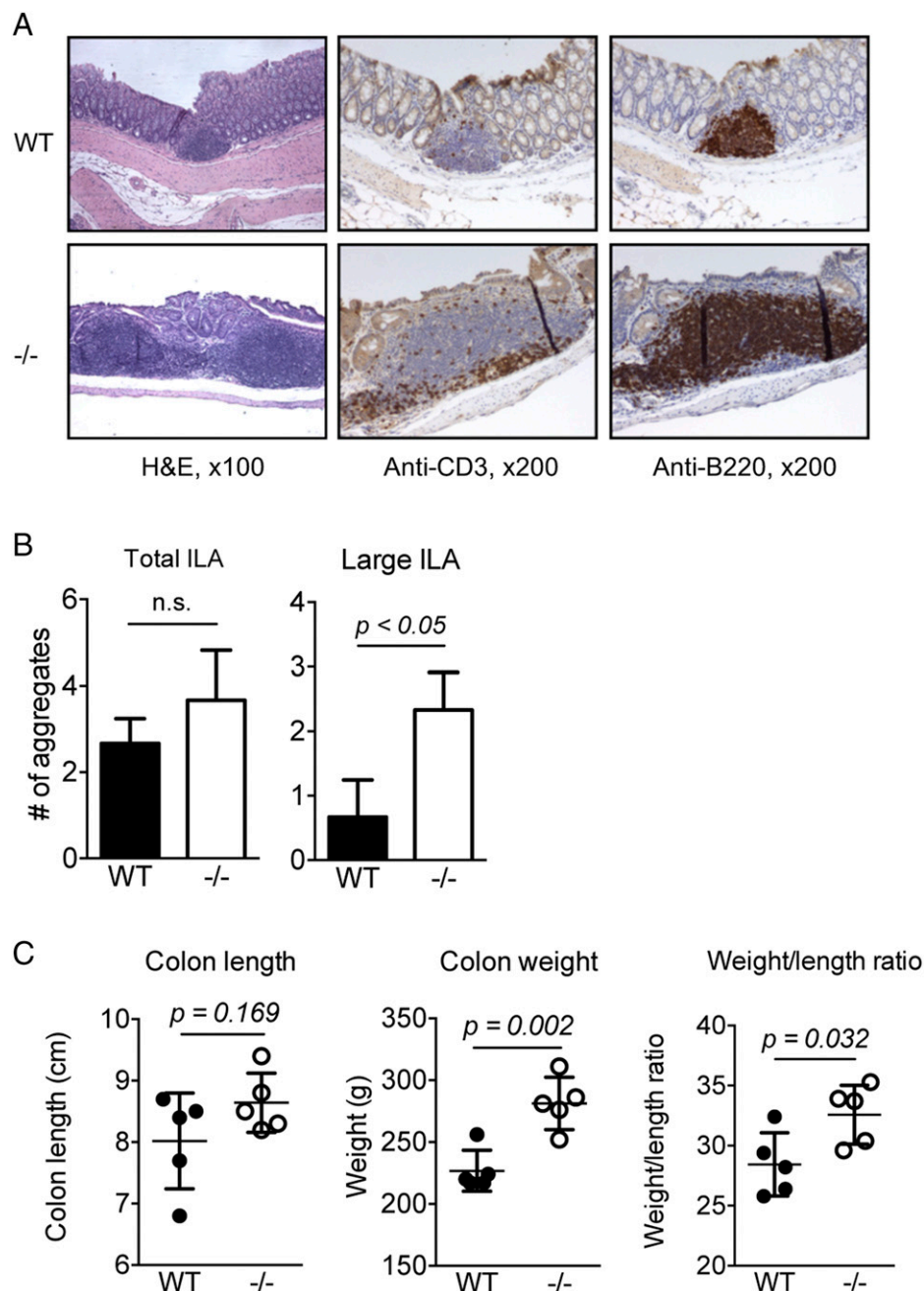
FIGURE 2. The colon of naive CRAMP$^{-/-}$ mice exhibits increased baseline inflammation. (**A**) WT and CRAMP$^{-/-}$ colons were histologically examined for the presence of ILAs ($n = 3$). (**B**) The number of total ILAs or large ILAs in the entire length of colon was counted. Data are mean $\pm$ SD of three mice. (**C**) The weight and the length of the colons were measured and the weight/length ratio was calculated. Data are mean $\pm$ SEM. Five mice were used for each group. n.s., not significant.

mild acute colitis with a higher disease activity index and mild mucosal leukocyte infiltration on day 5 of DSS treatment compared with WT mice (Fig. 5B). These results suggest that the increased susceptibility of CRAMP$^{-/-}$ mice to DSS may be dependent on the overgrowth of bacteria, but CRAMP may also protect mouse colon through additional mechanism(s) independent of its antimicrobial property.

The phenotype of CRAMP$^{-/-}$ mice is transferable to WT mice

To explore the possibility that CRAMP deficiency results in colonic dysbiosis, thereby enhancing the sensitivity to DSS-induced acute colitis, we cohoused WT and CRAMP$^{-/-}$ mice for 4 wk. As shown in Fig. 5C, the colon crypt length of untreated cohoused WT mice was reduced to the lengths in untreated CRAMP$^{-/-}$ mice, with decreased proliferating epithelial cells (Fig. 5D). Administration of 2% DSS for 5 d caused only minor disease activity in non-cohoused WT mice, whereas noncohoused CRAMP$^{-/-}$ mice

suffered severe acute colitis with a high mortality, as observed in earlier experiments (shown in Fig. 2). Interestingly, WT mice cohoused with CRAMP$^{-/-}$ mice showed signs of severe acute colitis with significant weight loss and 58% mortality (Fig. 5E, 5F). These results indicate that the high sensitivity of CRAMP$^{-/-}$ mice to DSS-induced colitis is transferable to WT mice by cohousing, presumably through the transfer of certain bacteria species that grow in the absence of CRAMP.

CRAMP deficiency alters the composition of microbiota in the colon

To determine whether CRAMP deficiency alters the composition of colonic microbiota in a naive state, as well as during DSS-induced colitis, we sequenced the DNA of microbiota in fecal pellets of mice. Fig. 6A shows a significantly different microbiota composition in noncohoused WT and noncohoused CRAMP$^{-/-}$ mice. After 4 wk of cohousing, the microbiota composition in the feces
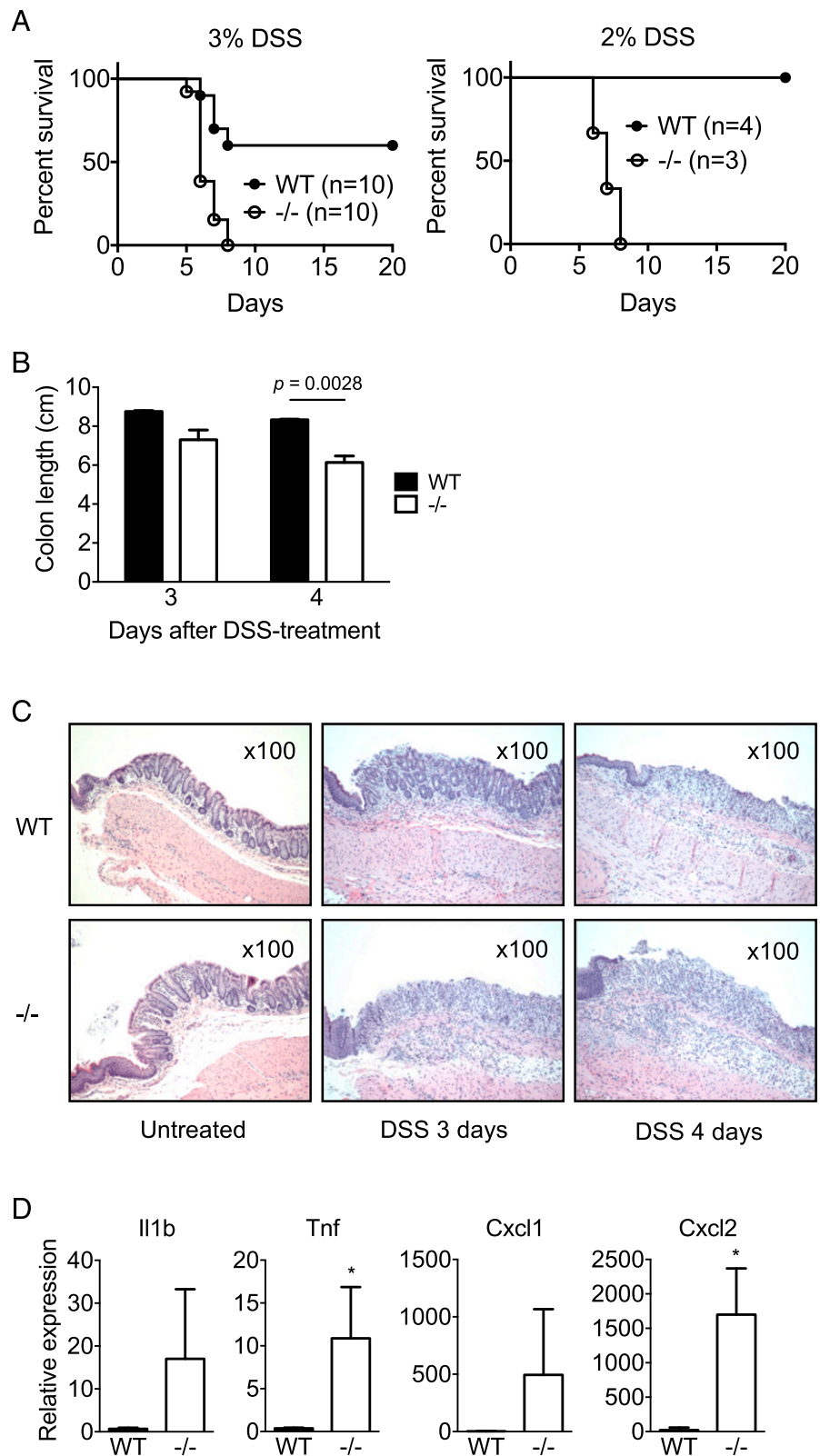
FIGURE 3. CRAMP$^{-/-}$ mice are highly sensitive to chemically induced acute colitis. (**A**) WT and CRAMP$^{-/-}$ mice were given 3 or 2% DSS in drinking water, and survival of mice was examined. (**B**) Colons were harvested from mice treated with 3% DSS on day 3 or 4, and their lengths were measured. Two mice per group for day 3 and three mice per group for day 4 were used. Data are mean ± SEM. (**C**) The distal section of colons from mice treated with 3% DSS was examined histologically using H&E staining (original magnification ×100). (**D**) The expression of IL-1β (Il1b), TNF-α (Tnf), CXCL1 (Cxcl1), and CXCL2 (Cxcl2) in the colon of mice treated with 3% DSS for 4 d was examined by real-time RT-PCR. Data are mean ± SD ($n = 3$ colons per group). *$p < 0.05$.

from WT mice shifted markedly toward that of CRAMP$^{-/-}$ mice. Treatment with DSS for 4 d revealed a clear difference in the microbiota composition between noncohoused WT mice and the other groups. A similar difference persisted at 21 and 56 d after DSS treatment.

A heat map was generated to show 45 bacteria strains in mouse feces (Fig. 6B) that exhibited statistically significant differences ($q < 0.1$) between samples, as determined by two-way ANOVA, using time posttreatment and mouse genotypes as factors. The heat map revealed that the majority of the changes in microbiota were caused by DSS treatment. Different species of bacteria were increased during the acute period of colitis in noncohoused WT and CRAMP$^{-/-}$ mice. In WT mice, the following bacterial populations were increased: *Mucispirillum schaedleri*, *Clostridium*
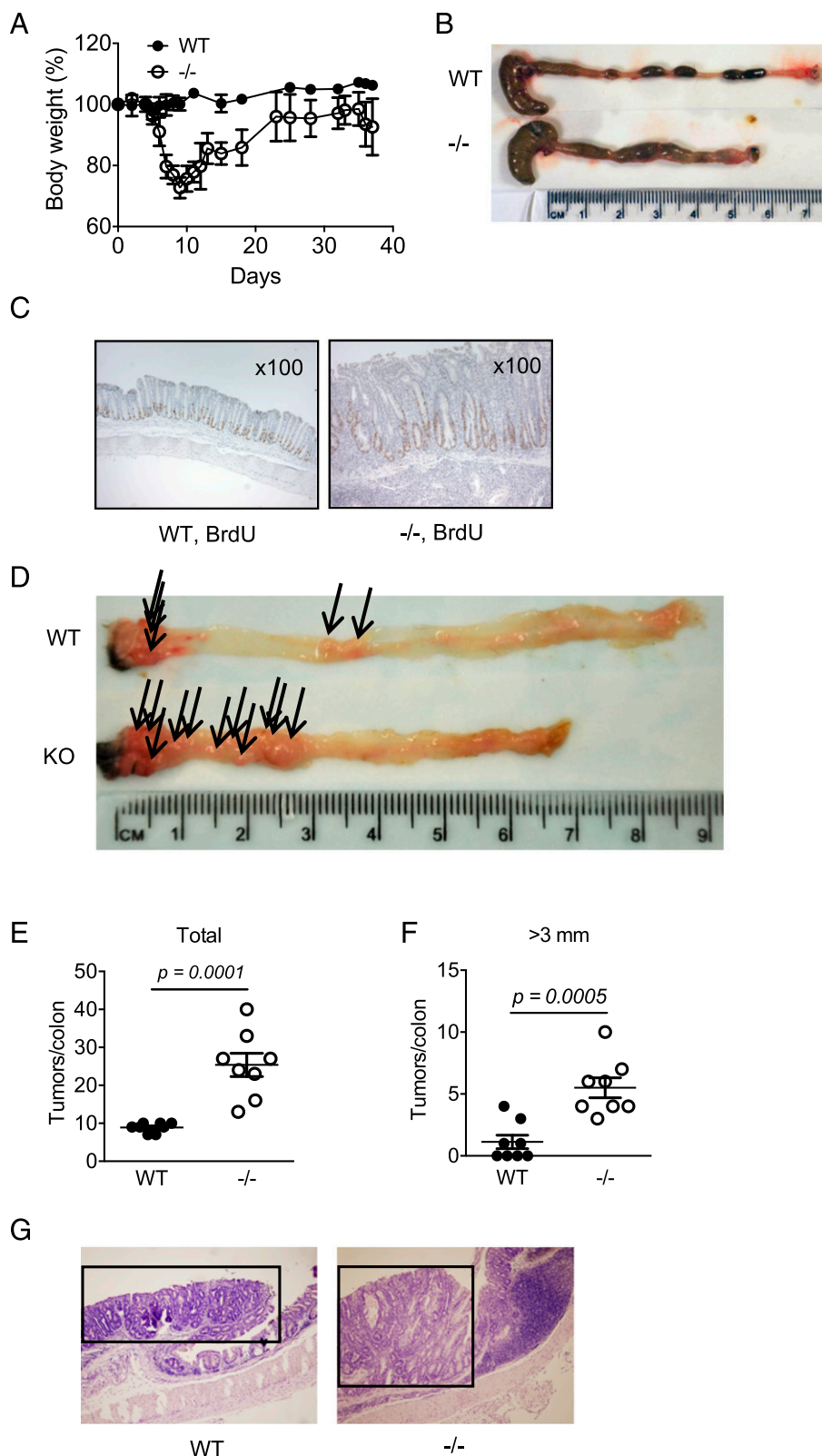
FIGURE 4. CRAMP$^{-/-}$ mice are highly sensitive to chemically induced chronic colitis and carcinogenesis. Mice were given 1.5% DSS for 5 d and were allowed to recover on regular water. On day 37, mice were euthanized, and colons were harvested. (**A**) Changes in body weight (%) are presented. (**B**) Mice were subjected to three cycles of 1.5% DSS treatment and euthanized on day 50. Colons were harvested, and the length was measured. (**C**) On day 20, 2 mg of BrdU was injected i.p. Twenty-four hours later, mice were euthanized, and the incorporation of BrdU into colon epithelial cells was examined by IHC. (**D–F**) The numbers and sizes of tumors that developed in the colon of eight WT mice and eight CRAMP$^{-/-}$ mice treated with AOM plus DSS were evaluated. The arrows in (D) indicate tumors. Data are mean ± SEM. (**G**) Tumors (outlined in boxes) that developed in the colon of WT and CRAMP$^{-/-}$ mice were examined histologically using H&E staining (original magnification ×100).

populeti, and *Acetivibrio cellulosolvens*. In CRAMP$^{-/-}$ mice, we saw an increase in *Odoribacter laneus*, *Ruminococcus lactaris*, *Desulfovibrio piger*, *Desulfomicrobium orale*, *Mogibacterium neglectum*, *Bacteroides acidifaciens*, and other species. The same bacterial species that increased during the acute phase of DSS

colitis in CRAMP$^{-/-}$ mice appear to be the ones that were transferred to WT mice during cohousing (Fig. 6B). This was evident by their significant increase in WT mice after cohousing with CRAMP$^{-/-}$ mice (Fig. 7). Among those species were bacteria typically found in oral microbiota, such as *M. neglectum* (23)
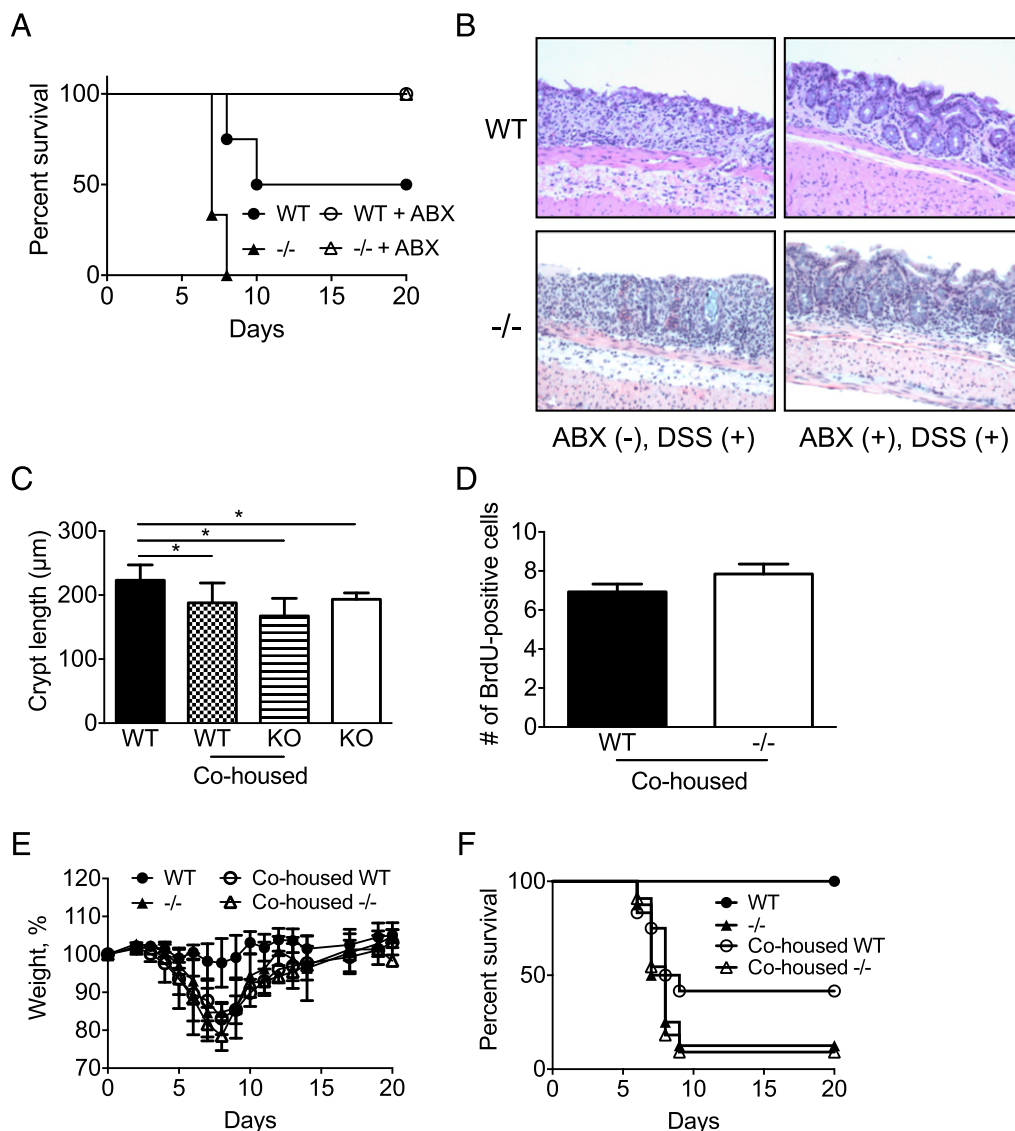
FIGURE 5. Severe DSS-induced colitis in CRAMP$^{-/-}$ mice is dependent on bacteria and is transferable. WT and CRAMP$^{-/-}$ were treated with a mixture of ABX (vancomycin, imipenem/cilastatin, and neomycin) for 3 wk and then administered 3% DSS in drinking water. (**A**) Survival of mice was examined. A representative of two experiments with similar results is presented. Three ABX-treated WT mice, five ABX-treated CRAMP$^{-/-}$ mice, three untreated WT mice, and three untreated CRAMP$^{-/-}$ mice were used. (**B**) One mouse from each group was euthanized, and the histological changes were examined in an H&E-stained section (original magnification ×200). (**C**) WT and CRAMP$^{-/-}$ mice were cohoused for 4 wk, and the crypt length was examined in H&E-stained sections. Data are mean ± SD. (**D**) To examine the proliferation of epithelial cells, mice were injected i.p. with 2 mg BrdU. Mice were euthanized 24 h after the injection, and incorporation of BrdU was detected by IHC. (**E** and **F**) Mice were given 3% DSS for 5 d in drinking water and allowed to recover. The change in body weight (**E**) and the survival (**F**) were monitored. Representative data of two experiments are shown for body weight (five noncohoused WT, five noncohoused CRAMP$^{-/-}$, eight cohoused WT, and seven cohoused CRAMP$^{-/-}$ mice were examined). Data are mean ± SEM. The summary of two experiments is shown for survival (9 noncohoused WT, 8 noncohoused CRAMP$^{-/-}$, 12 cohoused WT, and 10 cohoused CRAMP$^{-/-}$ mice were used). *$p < 0.05$.

and sulfate-reducing *D. piger a*nd *D. orale*; however, several known members of the gut microbiota, such as *O. laneus* and *R. lactaris*, also increased. After cohousing with CRAMP$^{-/-}$ mice, *O. laneus* increased in WT mice from almost undetectable levels to >10% of all bacteria in the fecal sample (Fig. 7). Moreover, DSS caused severe and persistent dysbiosis in all mice tested, which was reflected by a dramatic loss of bacterial species at different time points. Many bacterial species were already markedly decreased at day 4 post-DSS, including *Lactobacillus intestinalis* and *Candidatus arthromitus* (segmented filamentous bacteria), and some, including *Escherichia coli*, were lost at day 21 post-DSS treatment. Bacterial species that were downregulated during colitis were primarily from the genus *Clostridium*; how-

ever, their numbers recovered at later time points and returned to pre-DSS levels.

To obtain additional evidence supporting a role for CRAMP in the maintenance of microbiota in the colon, we generated WT and CRAMP$^{-/-}$ littermates by mating pairs of male and female heterozygous (CRAMP$^{+/-}$) mice and then single housed each littermate mouse, collected fecal pellets, and analyzed their colonic microbiota. As shown in Fig. 8A, the composition of fecal microbiota of WT pups and heterozygous parents was similar. In contrast, although the difference in the composition between CRAMP$^{-/-}$ and WT pups was small soon after weaning and single mouse housing, there was increasing divergence with time (Fig. 8A). These results indicate a critical role for CRAMP in the
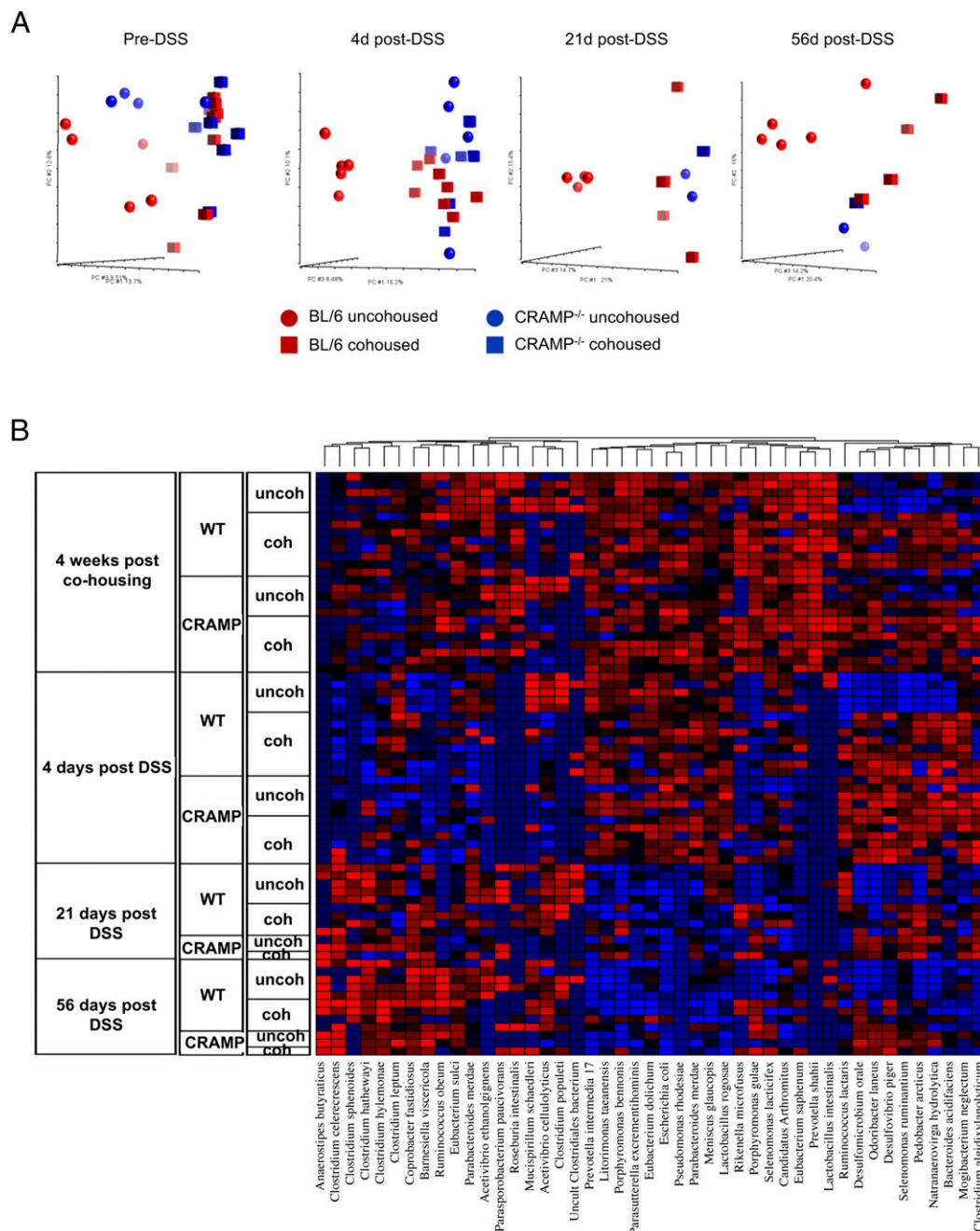
FIGURE 6. CRAMP deficiency alters the composition of microbiota in the colon. Fecal bacterial DNA was isolated from five noncohoused WT, five noncohoused CRAMP$^{-/-}$, eight cohoused WT, and six cohoused CRAMP$^{-/-}$ mice before and 4, 21, and 56 d after DSS treatment. On days 21 and 56, DNA was isolated from surviving mice. (**A**) Principal component analysis of unweighted UniFrac distances are visualized for different time points. (**B**) 16S sequence frequencies were analyzed by 16S amplicon high-throughput sequencing of fecal microbiota. Data are shown as a heat map of classified sequences (species level). Species were selected based on two-way ANOVA analysis using time and genotype as variables, followed by multiple tests correction ($q < 0.1$).

maintenance of a balanced microbiota in the colon and the potential involvement of bacteria expanded in the absence of the antimicrobial CRAMP in the severity of DSS colitis. It should be noted that bacterial species identified in single-housed WT and CRAMP$^{-/-}$ littermates (Fig. 8B) were different from those of earlier experiments (Fig. 6B), in which we focused on the species whose abundance changed after the induction of colitis in cohoused mice.

Discussion

Cathelicidins are a family of mammalian antimicrobial proteins that consist of an N-terminal putative signal peptide, a con-

served cathelin-like domain, and a C-terminal antimicrobial domain that varies remarkably in size (12–97 aa). More than 40 members of the cathelicidin family have been identified in different species; however, humans and mice each produce only one cathelicidin: human cationic antimicrobial protein 18 and the mouse ortholog, CRAMP, respectively. CRAMP$^{-/-}$ mice were previously demonstrated to develop more severe colitis than WT mice in response to DSS (24); however, the mechanistic basis of that observation remains unclear. In the current study, we revealed a novel role for CRAMP in colon mucosal homeostasis and provided a new mechanism by which
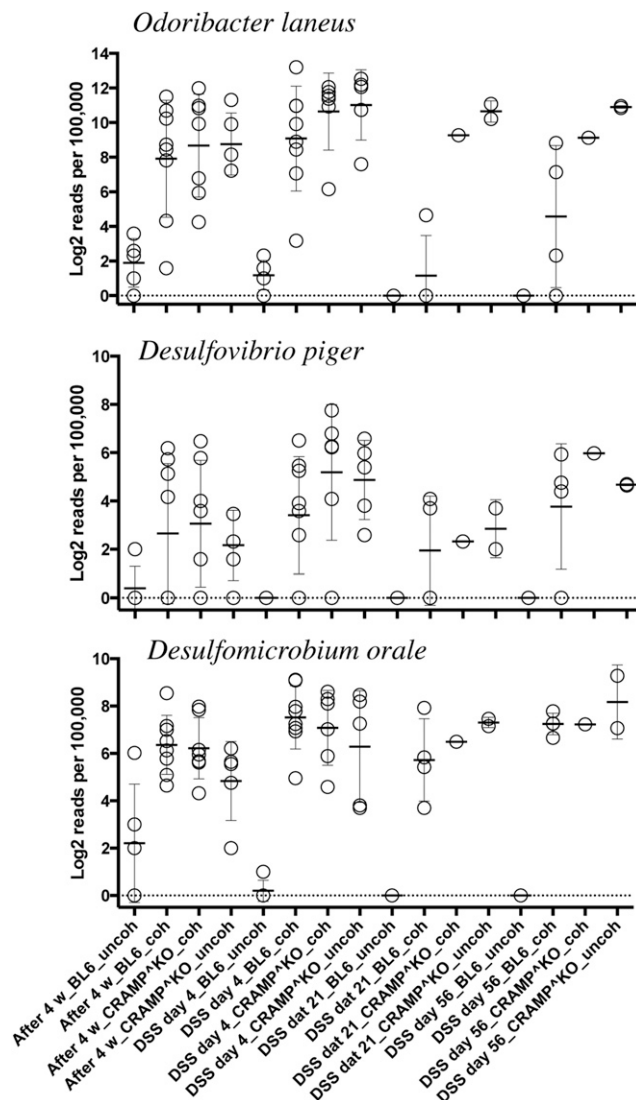
FIGURE 7. CRAMP deficiency alters the composition of certain bacteria in the colon. Three species (*O. laneus, D. piger*, and *D. orale*) whose frequencies were significantly increased after cohousing of WT mice with CRAMP$^{-/-}$ mice. The *x*-axis represents groups, and the *y*-axis represents the log2-transformed number of reads per 100,000 (typically sequenced per sample).

CRAMP protects mice from DSS-induced colitis and associated carcinogenesis.

It is now widely accepted that commensal bacteria are involved in the regulation of intestinal epithelial cell turnover, promotion of epithelial restitution, and reorganization of tight junctions, all of which are critical for fortifying barrier function; thus, microbial dysbiosis may cause pathological responses (1). In the current study, we revealed reduced proliferation of colon epithelial cells in CRAMP$^{-/-}$ mice, which was associated with increased susceptibility to DSS-induced colitis. We additionally showed that DSS-induced severe colitis in CRAMP$^{-/-}$ mice was partially preventable by ABX, and the colon phenotype found in CRAMP$^{-/-}$ mice was transferable to WT mice after cohousing. These observations were corroborated by a clear difference in the bacterial composition in the feces between noncohoused WT and CRAMP$^{-/-}$ mice, and cohousing of WT mice with CRAMP$^{-/-}$ mice dramatically shifted the bacterial composition in the feces of WT mice toward that of CRAMP$^{-/-}$ mice. Furthermore, the

colonic microbiota of CRAMP$^{-/-}$ mice diverged from that of littermate WT mice after single housing. Thus, CRAMP appears to play a critical role in the maintenance of healthy microbiota in the colon, as well as in the prevention of outgrowth of certain bacteria to cause severe colitis.

We noted an increase in several species of bacteria in WT mice after cohousing with CRAMP$^{-/-}$ mice, including *O. laneus*, *D. piger*, and *D. orale*, which likely transferred from CRAMP$^{-/-}$ mice. Because *M. neglectum*, *D. piger*, and *D. orale* are known components of the oral microbiota, and cathelicidins are found in salivary glands, the increase in those species in the colon of CRAMP$^{-/-}$ mice could be due to their overgrowth in the mouth. *D. piger* and *D. orale* are sulfate-reducing bacteria, and hydrogen sulfate has been implicated in the development of colitis (25). This emphasized the importance of CRAMP in the control of the balance of microbiota for disease prevention.

Cathelicidins are predominantly stored constitutively at high concentrations in the secondary granules of neutrophils, which, during the course of degranulation, release the C-terminal mature antimicrobial peptides (e.g., LL-37) by proteolytic cleavage. In addition to neutrophils, other leukocytes, including monocytes/macrophages, mast cells, and epithelial cells, generate cathelicidin, particularly in response to proinflammatory stimuli, including cytokines, pathogen-associated molecular patterns, or tissue injury (13). Koon et al. (24) demonstrated increased expression of CRAMP in the colon of mice with DSS-induced colitis. CRAMP expression was increased in the mucosal epithelium and in colonic macrophages, which appeared to be regulated by the interaction between TLR9 and genomic DNA of bacteria present in the colon. CRAMP from bone marrow (BM)-derived immune cells, especially macrophages, regulated DSS induction of colitis using mice transplanted with CRAMP$^{-/-}$ BM cells (24). We detected high-level expression of CRAMP mRNA and protein in BM cells from WT mice (Supplemental Fig. 1B, 1C). In addition, myeloid cell–specific CRAMP$^{-/-}$ mice were more sensitive to DSS-induced colitis than control mice (Supplemental Fig. 2); thus, our results are consistent with the notion that myeloid cell–derived CRAMP is critical for the control of colitis (24). However, deletion of CRAMP in intestinal epithelial cells also moderately increased the sensitivity to DSS, suggesting the participation of epithelium-derived CRAMP in colon homeostasis.

It is interesting to note that there are similarities in the phenotype between CRAMP$^{-/-}$ and Fpr2$^{-/-}$ mice in that they both show defects in colon mucosal development and repair (7). However, in contrast to Fpr2$^{-/-}$ mice, which showed decreased acute colitis syndrome upon intake of high-dose DSS and, therefore, a reduced acute mortality, CRAMP$^{-/-}$ mice developed more severe colitis and succumbed rapidly. Thus, in addition to sustaining colon mucosal homeostasis, which may be dependent on interaction with the receptor Fpr2, CRAMP actively controls pathogen overgrowth in the colon via its antimicrobial property, which causes severe colitis. Further research is ongoing to more precisely clarify the role of CRAMP and Fpr2 interactions in the pathophysiological process in the colon.

In addition to the phenotypes described above, we noted that CRAMP$^{-/-}$ mice consume more drinking water than WT mice in the naive state (data not shown), which is associated with the more severe acute colitis observed in CRAMP$^{-/-}$ mice after inflammatory stimulation. Therefore, we adjusted the concentration of DSS based on their water consumption so that WT and CRAMP$^{-/-}$ mice would take in equivalent doses of DSS. All CRAMP$^{-/-}$ mice still exhibited severe colitis and died by day 9, whereas all WT mice survived (data not shown). This confirms that CRAMP$^{-/-}$ mice are more sensitive to DSS-induced colonic inflammation. Similar to
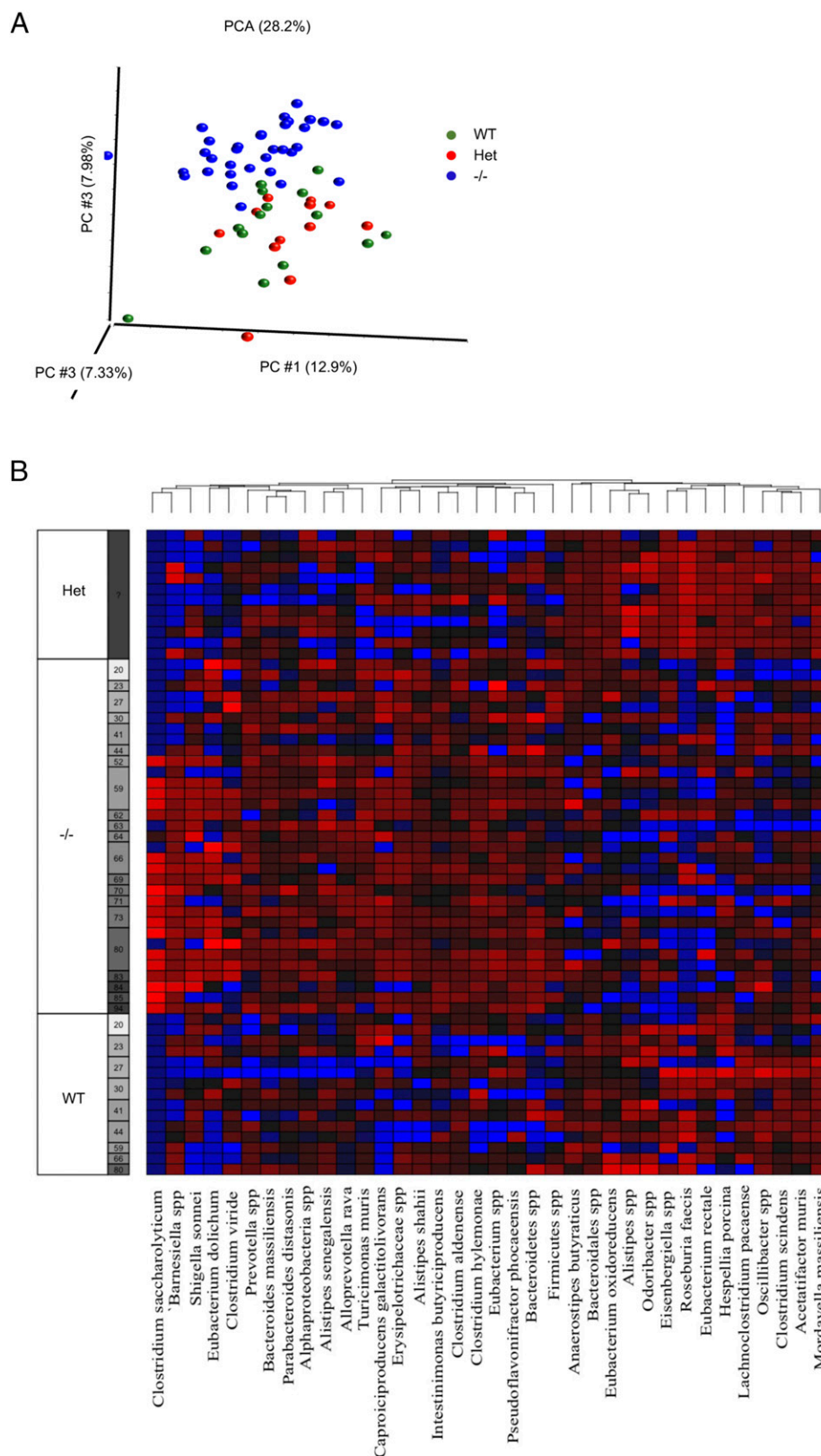
FIGURE 8. The colonic microbiota of CRAMP$^{-/-}$ mice diverges from that of littermate WT mice after single housing. (**A**) CRAMP heterozygotes (CRAMP$^{+/-}$) were generated by crossing CRAMP$^{-/-}$ mice to WT mice, and several cages of CRAMP$^{+/-}$ breeding pairs were set up. Pups were genotyped and weaned at 4 wk. WT or CRAMP$^{-/-}$ pups were single housed for up to 13 wk, and feces were collected to analyze the bacterial composition. Principal component analysis of unweighted UniFrac distances are visualized. (**B**) 16S sequence frequencies were analyzed by 16S amplicon high-throughput sequencing of fecal microbiota. Data are shown as a heat map of classified sequences (species level). Species were selected based on two-way ANOVA analysis using time and genotype as variables, followed by multiple tests correction ($q < 0.1$).

systemic CRAMP$^{-/-}$ mice, myeloid cell–specific, but not intestinal epithelial cell–specific, CRAMP$^{-/-}$ mice consumed greater volumes of drinking water than the control mice, an indication of their potential to suffer from more severe colitis.

In conclusion, CRAMP, among several antimicrobial peptides in the mammalian gut, plays a nonredundant role in mouse colon epithelial

homeostasis and inflammation. In addition to its antimicrobial activity against a broad range of Gram-positive and Gram-negative bacteria, as well as fungi, in vitro (26), CRAMP appears to control the growth of certain pathological bacteria in the colon. Further studies are required to more precisely define its role in the maintenance of microbiota in the gut and in the overall host interactions with the microbiota.

Acknowledgments

Disclosures

The authors have no financial conflicts of interest.

References

1. Yu, L. C., J. T. Wang, S. C. Wei, and Y. H. Ni. 2012. Host-microbial interactions and regulation of intestinal epithelial barrier function: from physiology to pathology. *World J. Gastrointest. Pathophysiol.* 3: 27–43.
2. Ishii, K. J., S. Koyama, A. Nakagawa, C. Coban, and S. Akira. 2008. Host innate immune receptors and beyond: making sense of microbial infections. *Cell Host Microbe* 3: 352–363.
3. Medzhitov, R. 2007. Recognition of microorganisms and activation of the immune response. *Nature* 449: 819–826.
4. Le, Y., P. M. Murphy, and J. M. Wang. 2002. Formyl-peptide receptors revisited. *Trends Immunol.* 23: 541–548.
5. Ye, R. D., F. Boulay, J. M. Wang, C. Dahlgren, C. Gerard, M. Parmentier, C. N. Serhan, and P. M. Murphy. 2009. International Union of Basic and Clinical Pharmacology. LXXIII. Nomenclature for the formyl peptide receptor (FPR) family. *Pharmacol. Rev.* 61: 119–161.
6. Li, L., K. Chen, Y. Xiang, T. Yoshimura, S. Su, J. Zhu, X. W. Bian, and J. M. Wang. 2016. New development in studies of formyl-peptide receptors: critical roles in host defense. *J. Leukoc. Biol.* 99: 425–435.
7. Chen, K., M. Liu, Y. Liu, T. Yoshimura, W. Shen, Y. Le, S. Durum, W. Gong, C. Wang, J. L. Gao, et al. 2013. Formylpeptide receptor-2 contributes to colonic epithelial homeostasis, inflammation, and tumorigenesis. *J. Clin. Invest.* 123: 1694–1704.
8. Schauber, J., D. Rieger, F. Weiler, J. Wehkamp, M. Eck, K. Fellermann, W. Scheppach, R. L. Gallo, and E. F. Stange. 2006. Heterogeneous expression of human cathelicidin hCAP18/LL-37 in inflammatory bowel diseases. *Eur. J. Gastroenterol. Hepatol.* 18: 615–621.
9. Kurosaka, K., Q. Chen, F. Yarovinsky, J. J. Oppenheim, and D. Yang. 2005. Mouse cathelin-related antimicrobial peptide chemoattracts leukocytes using formyl peptide receptor-like 1/mouse formyl peptide receptor-like 2 as the receptor and acts as an immune adjuvant. *J. Immunol.* 174: 6257–6265.
10. Ménard, S., V. Förster, M. Lotz, D. Gütle, C. U. Duerr, R. L. Gallo, B. Henriques-Normark, K. Pütsep, M. Andersson, E. O. Glocker, and M. W. Hornef. 2008. Developmental switch of intestinal antimicrobial peptide expression. *J. Exp. Med.* 205: 183–193.
11. Tai, E. K., W. K. Wu, H. P. Wong, E. K. Lam, L. Yu, and C. H. Cho. 2007. A new role for cathelicidin in ulcerative colitis in mice. *Exp. Biol. Med. (Maywood)* 232: 799–808.
12. Wong, C. C., L. Zhang, Z. J. Li, W. K. Wu, S. X. Ren, Y. C. Chen, T. B. Ng, and C. H. Cho. 2012. Protective effects of cathelicidin-encoding *Lactococcus lactis* in murine ulcerative colitis. *J. Gastroenterol. Hepatol.* 27: 1205–1212.
13. Yang, D., G. de la Rosa, P. Tewary, and J. J. Oppenheim. 2009. Alarmins link neutrophils and dendritic cells. *Trends Immunol.* 30: 531–537.
14. Wirtz, S., C. Neufert, B. Weigmann, and M. F. Neurath. 2007. Chemically induced mouse models of intestinal inflammation. *Nat. Protoc.* 2: 541–546.
15. Neufert, C., C. Becker, and M. F. Neurath. 2007. An inducible mouse model of colon carcinogenesis for the analysis of sporadic and inflammation-driven tumor progression. *Nat. Protoc.* 2: 1998–2004.
16. Iida, N., A. Dzutsev, C. A. Stewart, L. Smith, N. Bouladoux, R. A. Weingarten, D. A. Molina, R. Salcedo, T. Back, S. Cramer, et al. 2013. Commensal bacteria control cancer response to therapy by modulating the tumor microenvironment. *Science* 342: 967–970.
17. Laukoetter, M. G., P. Nava, W. Y. Lee, E. A. Severson, C. T. Capaldo, B. A. Babbin, I. R. Williams, M. Koval, E. Peatman, J. A. Campbell, et al. 2007. JAM-A regulates permeability and inflammation in the intestine in vivo. *J. Exp. Med.* 204: 3067–3076.
18. Kozich, J. J., S. L. Westcott, N. T. Baxter, S. K. Highlander, and P. D. Schloss. 2013. Development of a dual-index sequencing strategy and curation pipeline for analyzing amplicon sequence data on the MiSeq Illumina sequencing platform. *Appl. Environ. Microbiol.* 79: 5112–5120.
19. Smith, P. D., L. E. Smythies, R. Shen, T. Greenwell-Wild, M. Gliozzi, and S. M. Wahl. 2011. Intestinal macrophages and response to microbial encroachment. *Mucosal Immunol.* 4: 31–42.
20. Cesta, M. F. 2006. Normal structure, function, and histology of the spleen. *Toxicol. Pathol.* 34: 455–465.
21. Yeung, M. M., S. Melgar, V. Baranov, A. Oberg, A. Danielsson, S. Hammarström, and M. L. Hammarström. 2000. Characterisation of mucosal lymphoid aggregates in ulcerative colitis: immune cell phenotype and TcR-gammadelta expression. *Gut* 47: 215–227.
22. Perše, M., and A. Cerar. 2012. Dextran sodium sulphate colitis mouse model: traps and tricks. *J. Biomed. Biotechnol.* 2012: 718617.
23. Nakazawa, F., S. E. Poco, Jr., M. Sato, T. Ikeda, S. Kalfas, G. Sundqvist, and E. Hoshino. 2002. Taxonomic characterization of *Mogibacterium diversum* sp. nov. and *Mogibacterium neglectum* sp. nov., isolated from human oral cavities. *Int. J. Syst. Evol. Microbiol.* 52: 115–122.
24. Koon, H. W., D. Q. Shih, J. Chen, K. Bakirtzi, T. C. Hing, I. Law, S. Ho, R. Ichikawa, D. Zhao, H. Xu, et al. 2011. Cathelicidin signaling via the Toll-like receptor protects against colitis in mice. *Gastroenterology* 141: 1852–1863.e1–3.
25. Rowan, F. E., N. G. Docherty, J. C. Coffey, and P. R. O'Connell. 2009. Sulphate-reducing bacteria and hydrogen sulphide in the aetiology of ulcerative colitis. *Br. J. Surg.* 96: 151–158.
26. Travis, S. M., N. N. Anderson, W. R. Forsyth, C. Espiritu, B. D. Conway, E. P. Greenberg, P. B. McCray, Jr., R. I. Lehrer, M. J. Welsh, and B. F. Tack. 2000. Bactericidal activity of mammalian cathelicidin-derived peptides. *Infect. Immun.* 68: 2748–2755.